

ORIGINAL RESEARCH ARTICLE

Cardiac Reprogramming and Gata4 Overexpression Reduce Fibrosis and Improve Diastolic Dysfunction in Heart Failure With Preserved Ejection Fraction

Yu Yamada¹, MD*; Taketaro Sadahiro¹, MD, PhD*; Koji Nakano, MD; Seiichiro Honda¹, MD; Yuto Abe¹, MD; Tatsuya Akiyama¹, MD; Ryo Fujita¹, PhD; Masashi Nakamura¹, MD; Takashi Maeda¹, MD; Yuta Kuze; Masaya Onishi, PhD; Masahide Seki¹, PhD; Yutaka Suzuki, PhD; Chikara Takeuchi, PhD; Yuka W. Iwasaki¹, PhD; Kensaku Murano¹, PhD; Mamiko Sakata-Yanagimoto, MD, PhD; Shigeru Chiba¹, MD, PhD; Hideyuki Kato¹, MD, PhD; Hiroaki Sakamoto¹, MD, PhD; Yuji Hiramatsu¹, MD, PhD; Masaki Ieda¹, MD, PhD

BACKGROUND: Heart failure with preserved ejection fraction (HFpEF) is a major health concern. Pathological stimuli and interactions between cardiac fibroblasts (CFs) and other cell types may lead to cardiac fibrosis and diastolic dysfunction, which are hallmarks of HFpEF. Interstitial and perivascular cardiac fibrosis correlates with poor prognosis in HFpEF; however, mechanisms of fibrosis remain poorly elucidated, and targeted therapies are lacking. Cardiac reprogramming is a promising therapeutic approach for myocardial infarction that facilitates cardiac regeneration and antifibrosis action through *Mef2c/Gata4/Tbx5/Hand2* (MGTH) overexpression in resident CFs. However, the efficacy of this approach on HFpEF is yet to be established.

METHODS: Herein, we examined the effects of cardiac reprogramming in HFpEF using Tcf21^{iCre}/Tomato/MGTH2A transgenic mice, which expressed both MGTH and reporter expression in CFs for cardiac reprogramming and lineage tracing upon tamoxifen administration. To establish HFpEF model mice, we used a combination of a high-fat diet and nitric oxide synthase inhibition. Bulk RNA-sequencing, single-cell RNA-sequencing, and spatial transcriptomics were conducted to determine fibrotic mechanisms and the efficacy of cardiac reprogramming in HFpEF. We generated new tamoxifen-inducible transgenic mice overexpressing each reprogramming factor in CFs to investigate the effect of single factors. Last, we analyzed the effect of reprogramming factors in human CFs.

RESULTS: Cardiac reprogramming with MGTH overexpression improved diastolic dysfunction, cardiac hypertrophy, fibrosis, inflammation, and capillary loss in HFpEF. Cardiac reprogramming converted approximately 1% of resident CFs into induced cardiomyocytes. Bulk RNA-seq indicated that MGTH overexpression upregulated genes related to heart contraction and suppressed the fetal gene program (*Nppa* and *Nppb*) and proinflammatory and fibrotic signatures. Single-cell RNA-sequencing and spatial transcriptomics revealed that multiple CF clusters upregulated fibrotic genes to induce diffuse interstitial fibrosis, whereas distinct CF clusters generated focal perivascular fibrosis in HFpEF. MGTH overexpression reversed these profibrotic changes. Among 4 reprogramming factors, only Gata4 overexpression in CFs reduced fibrosis and improved diastolic dysfunction in HFpEF by suppressing CF activation without generating new induced cardiomyocytes. Gata4 overexpression also suppressed profibrotic signatures in human CFs.

CONCLUSIONS: Overexpressing Gata4 in CFs may be a promising therapeutic approach for HFpEF by suppressing fibrosis and improving diastolic dysfunction

Correspondence to: Masaki Ieda, MD, PhD, Department of Cardiology, Keio University School of Medicine, 35 Shinanomachi, Shinjuku-ku, Tokyo 160-8582, Japan. Email mieda@keio.jp

*Y. Yamada and T. Sadahiro contributed equally.

Supplemental Material is available at <https://www.ahajournals.org/doi/suppl/10.1161/CIRCULATIONAHA.123.067504>.

For Sources of Funding and Disclosures, see page XXX.

© 2024 American Heart Association, Inc.

Circulation is available at www.ahajournals.org/journal/circ

GRAPHIC ABSTRACT: A graphic abstract is available for this article.

Key Words: cardiac fibroblasts ■ fibrosis ■ heart failure ■ single-cell RNA-sequencing ■ spatial transcriptomics

Editorial, see p XXX

Clinical Perspective

What Is New?

- Cardiac reprogramming with *Mef2c/Gata4/Tbx5/Hand2* (MGTH) overexpression generated new induced cardiomyocytes, reduced fibrosis, attenuated diastolic dysfunction, and improved cardiac performance in heart failure with preserved ejection fraction (HFpEF).
- In HFpEF, profibrotic changes in multiple cardiac fibroblast (CF) clusters induced diffuse interstitial fibrosis, whereas distinct fibrogenic CF clusters contributed to focal perivascular fibrosis. Cardiac reprogramming reversed these profibrotic changes.
- Overexpression of Gata4 in CFs was sufficient to improve HFpEF and reduce fibrosis without generating induced cardiomyocytes. Gata4 overexpression suppressed CF activation by directly suppressing *Meox1*. Gata4 overexpression also suppressed profibrotic signatures in human CFs.

What Are the Clinical Implications?

- Cardiac fibrosis contributes to diastolic dysfunction and heart failure in HFpEF, and clinical therapies capable of effectively reversing fibrosis in HFpEF are currently unavailable.
- Gata4 overexpression can improve HFpEF by suppressing myocardial fibrosis and diastolic dysfunction.
- Overexpression of Gata4 in CFs may be a promising therapy for HFpEF.

Heat failure (HF) with preserved ejection fraction (HFpEF) accounts for approximately half the patients with HF worldwide and is increasing in prevalence, with mortality rates comparable to those of HF with reduced ejection fraction.¹ Several drug and device therapies have been shown to improve prognosis in patients with HF with reduced ejection fraction, but effective treatments for HFpEF remain markedly limited, resulting in an unmet clinical need.¹

In HFpEF pathogenesis, cardiac hypertrophy, inflammation, metabolic stress, and endothelial dysfunction may cooperate to induce left ventricular (LV) diastolic dysfunction and fibrosis, leading to a vicious cycle of functional impairment.^{1,2} Cardiac fibrosis is clinically present in most cases of HFpEF,³ and the extracellular

Nonstandard Abbreviations and Acronyms

CF	cardiac fibroblast
ECM	extracellular matrix
EC	endothelial cell
FACS	fluorescence-activated cell sorting
HF	heart failure
HFpEF	heart failure with preserved ejection fraction
iCM	induced cardiomyocyte
L-NAME	N-nitroarginine methyl ester
LV	left ventricle
MGTH	<i>Mef2c/Gata4/Tbx5/Hand2</i>
MI	myocardial infarction
RT-qPCR	reverse-transcription quantitative polymerase chain reaction
scRNA-seq	single-cell RNA sequencing
SeV	Sendai virus vector
TGFβ	transforming growth factor β
TTg	triple transgenic

matrix (ECM) burden strongly correlates with diastolic dysfunction and poor prognosis.⁴ Therefore, fibrosis can be a promising target for HFpEF; however, effective therapeutic strategies to address cardiac fibrosis are lacking.

The heart comprises various cell types, including cardiomyocytes, cardiac fibroblasts (CFs), endothelial cells (ECs), smooth muscle cells (SMCs), and immune cells.⁵ Single-cell RNA sequencing (scRNA-seq) has demonstrated that CFs comprise heterogeneous populations.^{6,7} After myocardial infarction (MI), resident CFs differentiate into myofibroblasts and matrifibrocytes, which secrete ECM to form extensive scar tissue (replacement fibrosis) to prevent ventricular wall rupture.^{8–11} In contrast, chronic stress conditions, including HFpEF, exhibit different fibrosis types, such as interstitial and perivascular fibrosis; however, the cellular and molecular mechanisms underlying these types of fibrosis remain unclear.¹² Moreover, as ECM deposit levels in patients with HFpEF are typically mild to moderate, whether antifibrotic treatment could improve diastolic dysfunction and cardiac performance in HFpEF remains unknown.^{4,13}

Direct cardiac reprogramming reportedly converted CFs into cardiomyocytes through *Mef2c/Gata4/Tbx5/Hand2*

(MGTH) overexpression *in vitro*. *In vivo*, cardiac reprogramming targeting resident CFs was found to restore cardiac function in acute and chronic MI through myocardial regeneration and antifibrotic effects.^{14–17} However, the impact of cardiac reprogramming on HFpEF remains unclear. Therefore, we examined the efficacy of cardiac reprogramming and the fibrotic mechanisms in an experimental model of HFpEF using multitranscriptomics, including bulk RNA-sequencing (RNA-seq), scRNA-seq, and spatial transcriptomics.

METHODS

For a detailed description of the methods, please see the [Supplemental Methods](#) section in the [Supplemental Material](#). All animal experiments conducted in this study were approved by the Tsukuba University ethics committees for animal experiments. All sequencing data are available from gene expression omnibus under Super-Series reference No. GSE218761.

Statistical Analysis

Statistical analyses are described in detail in the [Supplemental Methods](#) section in the [Supplemental Material](#). Statistical parameters, including the number of samples (n), descriptive statistics (mean and SEM), and significance, are indicated in the figures and figure legends. Statistical significance was set as $P < 0.05$.

RESULTS

Cardiac Reprogramming Reversed Diastolic Dysfunction in HFpEF

We used our newly developed Tcf21^{Cre}/Tomato/MGTH2A triple transgenic (TTg) mouse system, wherein treatment with tamoxifen can induce cardiac reprogramming in resident CFs, to determine the effect of cardiac reprogramming in HFpEF (Figure 1A).¹⁴ In TTg mice, tamoxifen treatment induced MGTH and Tomato expression in the CFs for cardiac reprogramming and lineage tracing (Figure 1A through 1C). Reverse-transcription quantitative polymerase chain reaction analyses confirmed that MGTH was significantly upregulated in the fluorescence-activated cell sorting–sorted Tomato⁺ cells in the TTg hearts compared with that in control mice (Ctrl, Tcf21^{Cre}/Tomato; Figure 1B; [Figure S1A through S1D](#)). The body weight, blood pressure, and cardiac performance (determined by echocardiography, cardiac catheterization, and treadmill test) in TTg mice fed normal chow (TTg-chow) were comparable to those of Ctrl mice fed normal chow (Ctrl-chow), suggesting that MGTH expression alone did not induce any phenotypic change in mice (Figure 1D through 1K; [Figure S1E through S1H](#)). Ctrl and TTg mice were then subjected to a well-characterized “2-hit” HFpEF model induced by a high-fat diet (HFD) and nitric oxide synthase inhibition using the

N-nitroarginine methyl ester (L-NAME) combination (Figure 1D).^{12,18} Five weeks of HFD+L-NAME feeding can sufficiently induce HFpEF in mice.^{12,18} HFD+L-NAME feeding triggered obesity and hypertension in Ctrl and TTg mice compared with mice fed normal chow (Ctrl-chow and TTg-chow) (Figure 1E).

Echocardiography revealed HFpEF phenotypes, including LV diastolic dysfunction indicated by elevated E/A and E/E', and preserved LV ejection fraction in Ctrl and TTg mice treatment with HFD+L-NAME for 5 weeks (Figure 1F and 1G). Interstitial and perivascular fibrosis were detected in HFpEF ventricles, colocalized with Tomato⁺ CFs (Figure 1C). After induction of HFpEF for 5 weeks, mice were treated with tamoxifen for 5 days to induce cardiac reprogramming to determine HFpEF phenotype reversal (Figure 1D). We sequentially analyzed 4 mouse groups: Ctrl-chow, TTg-chow, Ctrl mice fed HFD+L-NAME (Ctrl-HFpEF), and TTg mice fed HFD+L-NAME (TTg-HFpEF). MGTH overexpression did not affect food intake, and mice remained obese and hypertensive with preserved cardiac contractility for 15 weeks in the Ctrl-HFpEF and TTg-HFpEF groups (Figure 1E and 1G; [Figure S1E through S1H](#)). In contrast, echocardiographic evaluation revealed that LV diastolic dysfunction was significantly improved in TTg-HFpEF mice when compared with that in Ctrl-HFpEF mice at 10 and 15 weeks (Figure 1F and 1G). Consistent with improved diastolic function at 15 weeks, LV wall hypertrophy and diastolic velocity (E' wave) were also improved in TTg-HFpEF mice ([Figure S1F through S1H](#)). Cardiac catheterization indicated that LV end-diastolic pressure and end-diastolic pressure-volume relationship, hallmarks of HFpEF, were significantly elevated in the Ctrl-HFpEF mice compared with those in the Ctrl-chow mice at 15 weeks, although they were improved in TTg-HFpEF mice (Figure 1H and 1I). Furthermore, the treadmill test demonstrated that exercise tolerance, evaluated by running distance, was improved in TTg-HFpEF mice at 15 weeks (Figure 1J and 1K). These results suggest that cardiac reprogramming reversed LV diastolic dysfunction and improved cardiac function in HFpEF.

Cardiac Reprogramming Ameliorated Cardiac Hypertrophy, Fibrosis, Microvascular Rarefaction, and Inflammation in HFpEF

We next analyzed the pathological changes in the hearts of Ctrl-chow, TTg-chow, Ctrl-HFpEF, and TTg-HFpEF mice at 15 weeks. The heart weight/tibia length ratio and cardiomyocyte cross-sectional area were significantly increased in Ctrl-HFpEF mice compared with those in Ctrl- and TTg-chow mice, whereas they were decreased in the TTg-HFpEF group, suggesting that MGTH overexpression suppressed cardiac hypertrophy in HFpEF (Figure 2A through 2D). ECM deposition, as determined by

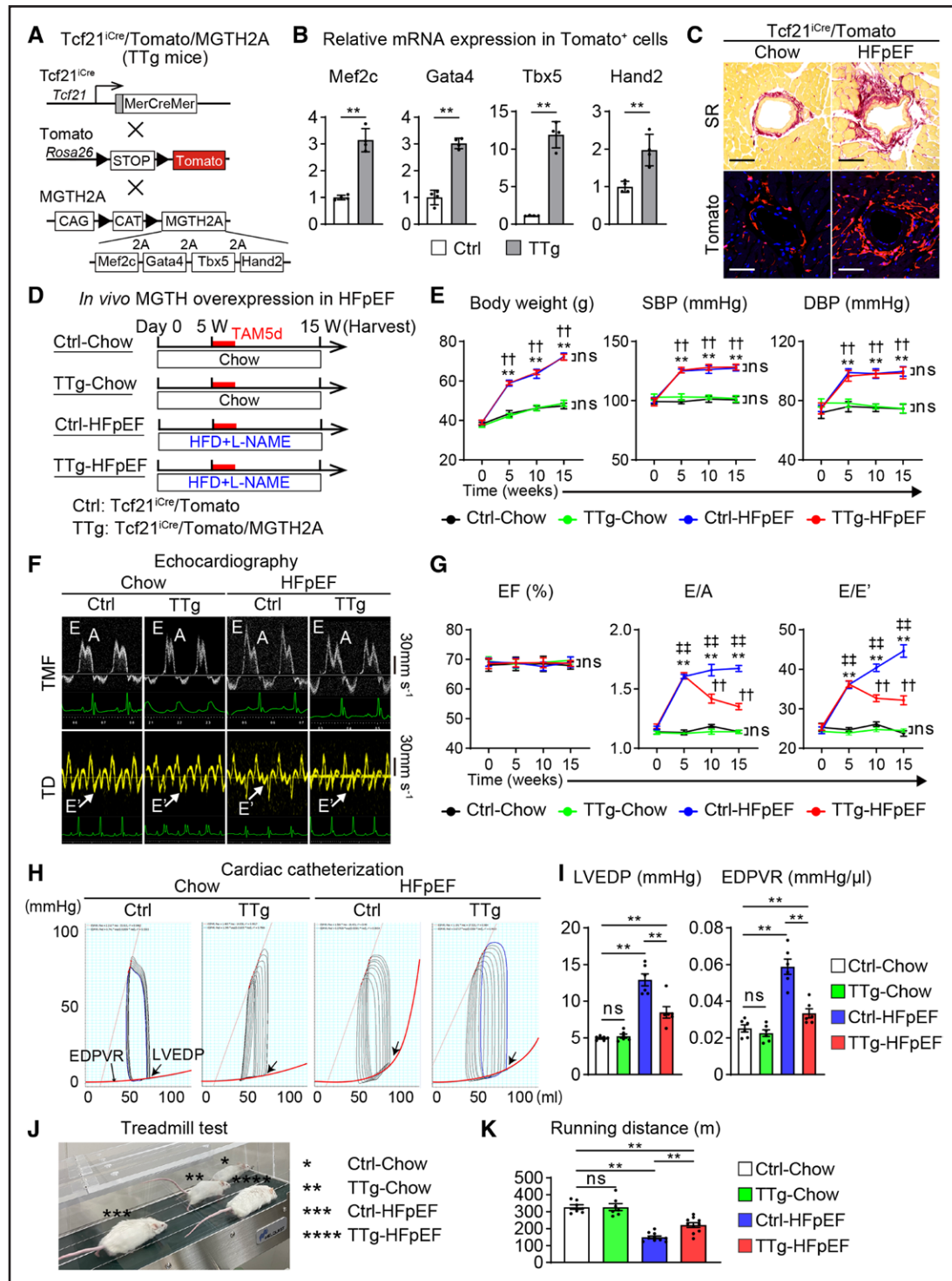


Figure 1. Cardiac reprogramming improves diastolic dysfunction in HFpEF.

A, Schematic representation of the strategy for *in vivo* MGTH2A overexpression in cardiac fibroblasts (CFs) using triple transgenic (TTg, *Tcf21*^{Cre}/Tomato/MGTH2A) mice generated by crossing MGTH2A mice with *Tcf21*^{Cre}/Tomato mice. **B**, Relative mRNA expression of *Mef2c*, *Gata4*, *Tbx5*, and *Hand2* in fluorescence-activated cell sorting (FACS)-sorted Tomato⁺ cells in control littermates (Ctrl, *Tcf21*^{Cre}/Tomato) and TTg mice 7 days after tamoxifen (TAM) administration (n=4 independent biological replicates). **C**, Representative images of hearts from *Tcf21*^{Cre}/Tomato mice with Sirius red (SR) staining and immunohistochemistry with Tomato and DAPI after 15 weeks of normal diet (Chow) or high-fat diet (HFD) + L-NAME treatment (HFpEF). Tomato⁺ cells are present in the perivascular fibrotic areas. TAM administration was performed as shown in **D**. **D**, Experimental strategy for MGTH2A overexpression in HFpEF. As indicated, Ctrl and TTg mice were fed with Chow or HFD+L-NAME treatment. TAM administration was initiated 5 weeks after treatment, and hearts were harvested 15 weeks after treatment (10 weeks after TAM administration). **E**, Body weight, systolic blood pressure (SBP), and diastolic blood pressure (DBP) were measured every 5 weeks for 15 weeks in Ctrl-chow (black line, n=7), TTg-chow (green line, n=7), Ctrl-HFpEF (blue line, n=10), and TTg-HFpEF (red line, n=10) mice. **F**, Representative (Continued)

Figure 1 Continued. echocardiographic tracings of pulsed wave Doppler of transmitral flow (TMF, **top**) and tissue Doppler (TD, **bottom**). The peak E wave velocity (E), peak A wave velocity (A), and peak E' wave velocity (E') are displayed. **G**, Left ventricular ejection fraction (EF), E/A ratio, and E/E' ratio of Ctrl-chow (black line, n=7), TTg-chow (green line, n=7), Ctrl-HFpEF (blue line, n=10), and TTg-HFpEF (red line, n=10) mice were measured using echocardiography every 5 weeks for a total of 15 weeks. **H** and **I**, Representative left ventricular pressure-volume loops recorded by cardiac catheterization (**H**). Arrows indicate the left ventricular end-diastolic pressure (LVEDP), and red lines indicate the end-diastolic pressure-volume relationship (EDPVR). Quantitative analyses are shown in **I** (n=6 independent biological replicates). **J** and **K**, Exercise tolerance was evaluated based on the running distance on a treadmill test (**J**). *Ctrl-chow; **TTg-chow; ***Ctrl-HFpEF; ****TTg-HFpEF. Quantitative analysis is shown in **K** (Ctrl-chow n=7; TTg-chow n=7; Ctrl-HFpEF, n=10; TTg-HFpEF, n=10). All data are presented as the mean±SEM. ** $P<0.01$ vs the relevant control using Student *t* test (**B**) and 1-way ANOVA followed by Tukey multicomparisons test (**I** and **K**). ** $P<0.01$ vs Ctrl-chow; †† $P<0.01$ vs Ctrl-chow; ‡‡ $P<0.01$ vs TTg-HFpEF using 2-way ANOVA followed by Tukey multicomparisons test (**E** and **G**). ns, Not significant. Scale bars=50 μ m. HFpEF indicates heart failure with preserved ejection fraction; and SEM, standard error of the mean.

Sirius red staining, revealed that cardiac fibrosis in TTg-HFpEF mice was significantly reduced compared with that in Ctrl-HFpEF mice at 15 weeks (Figure 2E and 2F). BrdU staining revealed that the number of BrdU⁺ proliferative CFs was significantly reduced in TTg-HFpEF mice compared with Ctrl-HFpEF, whereas the number of TUNEL⁺ apoptotic CFs was unchanged, thereby suggesting that reduced CF proliferation may contribute to regression of fibrosis (Figure S2A through S2D). Based on the immunohistochemistry analysis, the number of CD45⁺ inflammatory cells in the LV was significantly reduced in the TTg-HFpEF mice when compared with that in the Ctrl-HFpEF mice (Figure S2E and S2F). The capillary density, as determined by isolectin B4 staining, was reduced in Ctrl-HFpEF mice compared with that in Ctrl- and TTg-chow mice and significantly improved in TTg-HFpEF mice (Figure 2G and 2H). These results are consistent with the observed physiological improvement (Figure 1). Thus, MGTH overexpression in resident CFs ameliorated pathological changes induced in HFpEF ventricles.

To determine whether fibrosis facilitated the diastolic dysfunction observed in the HFpEF model, we analyzed the level of cardiac fibrosis and E/E' determined by echocardiography in 10-week Ctrl-HFpEF mice. A statistically significant correlation was observed between the 2 parameters (Figure S3A). Ctrl-HFpEF mice exhibited increased cardiac fibrosis at 5 weeks, which further increased thereafter, in line with the time course of diastolic dysfunction shown by echocardiography (Figure 1G; Figure S3B). Conversely, treatment with tamoxifen significantly decreased fibrosis in TTg-HFpEF mice, concordant with the improved diastolic dysfunction (Figure 1G; Figure S3B).

Subsequent evaluation of cardiac reprogramming and regeneration in TTg-HFpEF mice revealed that approximately 1% of Tomato⁺ cells expressed the cardiac marker of α -actinin, suggesting generation of induced cardiomyocytes (iCMs) in HFpEF, albeit with low efficiency (Figure 2I and 2J). Approximately half the iCMs were mature-type cardiomyocytes with clear sarcomeric structures (Figure S2G and S2H). We did not observe adverse effects, such as cardiac hypertrophy and hyperplasia, in TTg-chow and TTg-HFpEF mice (Figure 2A through 2D). Thus, MGTH overexpression in CFs improved HFpEF by

ameliorating cardiac hypertrophy, fibrosis, inflammation, and endothelial rarefaction, and inducing iCM generation.

Cardiac Reprogramming Upregulated Myocardial-Related Genes and Suppressed Fibrotic and Inflammatory Signatures in HFpEF

To identify molecular changes induced by cardiac reprogramming in HFpEF, we then used bulk RNA-seq to detect global gene expression profiles in Ctrl-chow, Ctrl-HFpEF, and TTg-HFpEF mouse ventricles at 15 weeks (Figure 3A). Differential gene expression and Gene Ontology analyses revealed that gene clusters upregulated in Ctrl-HFpEF mice, compared with those in Ctrl-chow mice, were enriched in fibrosis (supramolecular fiber and ECM organization) and inflammatory signatures (cytokine-mediated signaling pathway and regulation of inflammatory response). These upregulated genes in Ctrl-HFpEF mice were primarily suppressed in TTg-HFpEF mouse ventricles (Figure 3B). Compared with those in Ctrl-chow mice, gene clusters downregulated in Ctrl-HFpEF mice were enriched in cardiac function (regulation of heart contraction and ion transmembrane transport), which were primarily restored in TTg-HFpEF mice. Consistently, relative mRNA expression analyses confirmed that gene expression related to fibrosis (*Ccn2* and *Tgfb2*), inflammation (*Ccl2*, *Ccl7*, *Cx3cl1*, *Il6*, *Il33*, *Icam1*, and *Sele*), cardiac hypertrophy (*Acta1* and *Ankrd1*), and the fetal gene program induced by cardiac stress (*Nppa* and *Nppb*) was upregulated in Ctrl-HFpEF mice and suppressed in TTg-HFpEF mice (Figure 3C; Figure S4A and S4B). Therefore, in vivo cardiac reprogramming upregulated myocardial-related genes and suppressed fibrotic and inflammatory profiles in HFpEF to improve cardiac performance.

Given that MGTH were exclusively expressed in CFs in TTg-HFpEF ventricles, we analyzed the molecular signatures in cardiac interstitial cells, including CFs, using scRNA-seq (Figure 3A and 3D; Figure S5A).¹⁴ After quality control filtering, we acquired 36786 single-cell transcriptional data sets from the Ctrl-chow, Ctrl-HFpEF, and TTg-HFpEF groups (n=2 for each ventricle; Figure 3D). Unsupervised clustering of the scRNA-seq data revealed 9 populations, including CFs, mural cells/smooth muscle cells, ECs, macrophages, granulocytes,

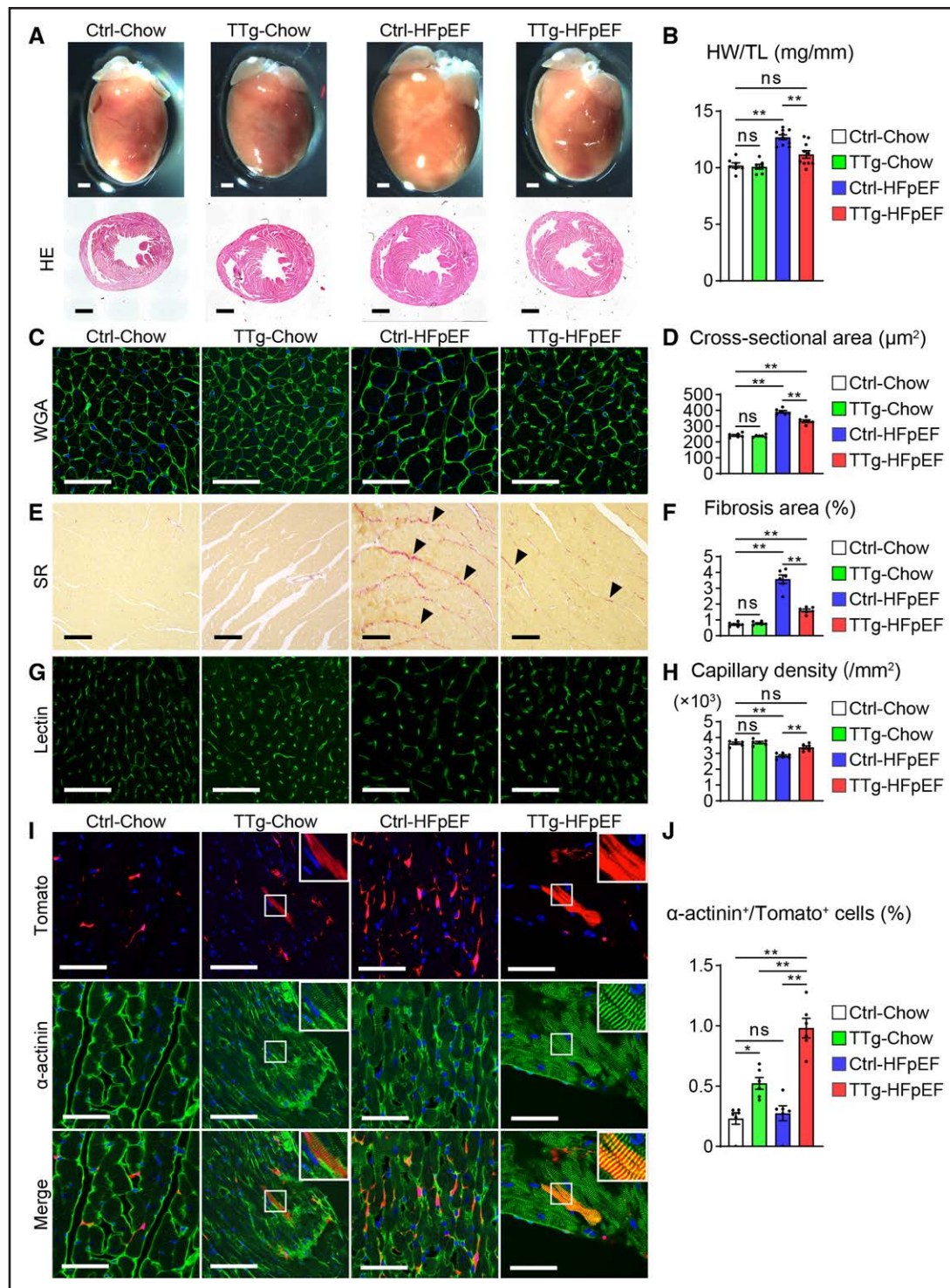


Figure 2. Cardiac reprogramming ameliorates histopathological changes and generates induced cardiomyocytes in HFpEF.

A, Mouse hearts at 15 weeks. **Bottom**, Hematoxylin-eosin (HE) staining. **B**, Ratio of heart weight (HW) to tibia length (TL; Ctrl-chow n=7; TTg-chow n=7; Ctrl-HFpEF, n=10; TTg-HFpEF, n=10). **C** and **D**, Immunohistochemistry for wheat germ agglutinin (WGA) staining of the left ventricle at 15 weeks (**C**). Quantitative analysis of cardiomyocyte cross-sectional area is shown in **D** (n=6 independent biological replicates). **E** and **F**, Representative images of Sirius red (SR) staining of the left ventricle at 15 weeks (**E**). The black arrowheads indicate the fibrosis area. Quantitative analysis of the fibrosis area is shown in **F** (n=6 independent biological replicates). **G** and **H**, Immunohistochemistry for isolectin B4 (Lectin) staining of the left ventricle at 15 weeks (**G**). Quantitative analysis of capillary density is shown in **H** (n=6 independent biological replicates). **I** and **J**, Immunohistochemistry for Tomato, α -actinin, and DAPI at 15 weeks (**I**). High-magnification views in insets show the sarcomeric organization in TTg-HFpEF. Quantitative analysis of α -actinin⁺/Tomato⁺ cells is shown in **J** (n=6 independent biological replicates). All data are presented as the mean \pm SEM. * P <0.05; ** P <0.01; vs the relevant control using 1-way ANOVA followed by Tukey multicomparisons test. ns, Not significant. Scale bars represent 1 mm (**A**), 100 μm (**E**), and 50 μm (**C**, **G**, and **I**). HFpEF indicates heart failure with preserved ejection fraction; and SEM, standard error of the mean.

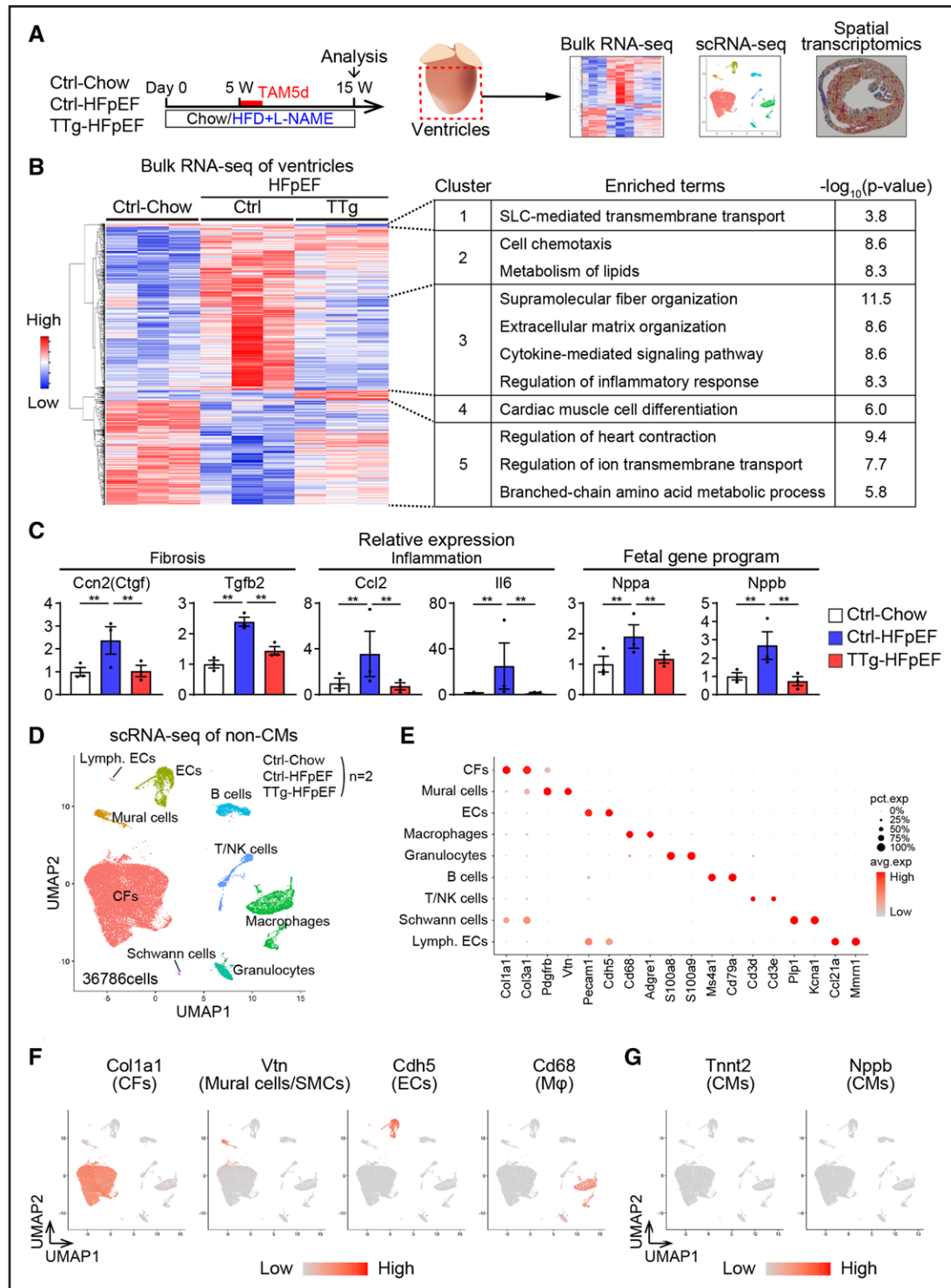


Figure 3. Cardiac reprogramming alters the transcriptional signatures in HFpEF.

A, Experimental workflow and analysis for bulk RNA-sequencing, single-cell RNA sequencing (scRNA-seq), and spatial transcriptomics. Ventricles were harvested at 15 weeks. **B**, Hierarchical clustering analysis of differentially expressed genes by bulk RNA-seq in the ventricles at 15 weeks ($n=3$ independent biological replicates). Selected GO terms for each cluster are also shown. **C**, Relative mRNA expression of fibrosis-, inflammation-, and heart failure-related genes in bulk RNA-seq data. **D**, Uniform manifold approximation and projection (UMAP) of scRNA-seq data integrating 36 786 single noncardiomyocytes (CMs) from Ctrl-chow, Ctrl-HFpEF, and TTg-HFpEF mice ventricles ($n=2$ per group). Nine clusters indicated by colors are marked with the presumed cell types. **E**, Dot plot visualization of representative marker genes used to identify clusters. The color and size of dots indicate the relative average expression level in each population and the percentage of cells expressing the gene, respectively. **F**, Expression of non-CM marker genes (*Col1a1*, *Vtn*, *Cdh5*, and *Cd68*) as visualized on UMAP plots. **G**, Expression of CM marker genes (*Tnnt2* and *Nppb*) as visualized on UMAP plots. All data are presented as the mean \pm SEM. ** $P < 0.01$, empirical analysis of differential gene expression in bulk RNA-seq. GO indicates Gene Ontology; HFpEF, heart failure with preserved ejection fraction; and SEM, standard error of the mean.

B cells, T/natural killer cells, Schwann cells, and lymphatic ECs (Figure 3D through 3F; Figure S5B through S5D).^{8,9} *Tcf21* and *Tomato* expression was limited to the CF cluster (Figure S5D). Cardiomyocyte-specific gene expression was not detected, suggesting that the isolated cells did not contaminate cardiomyocytes and iCMs (Figure 3G). CellChat analysis revealed ligand-receptor interactions between CFs and other interstitial cells, including inflammatory cells, ECs, and lymphatic ECs (Figure S5E and S5F).¹⁹ Among them, CFs were predicted to interact with ECs and lymphatic ECs through the VEGF-VEGFR, Ptn-Scd1, Mdk-Ncl, Cxcl12-Ackr3, and Angptl4-Cdh5 pathways. These results suggest that CFs interact with other interstitial cells in the ventricles, leading to changes in capillary density and inflammation.

Cardiac Reprogramming Suppressed Profibrotic Signatures in Multiple CF Clusters in HFpEF

To identify cellular and molecular changes induced in CFs in HFpEF and cardiac reprogramming, we then focused on CF clusters in the Ctrl-chow, Ctrl-HFpEF, and TTg-HFpEF groups (each n=2) using scRNA-seq. Unsupervised clustering revealed 6 clusters in the CF population (Figure 4A and 4B; Figure S6A and S6B). Uniform manifold approximation and projection revealed that *Col1a1*, *Tcf21*, and *Tomato* were universally expressed in CF clusters (Figure 4C). Gene Ontology analysis based on the cluster marker genes demonstrated that CF1 was associated with ECM organization, CF2 was associated with response to interferon β , and CF3 was associated with cellular stress response, whereas CF1 to 3 all expressed *Hsd11b1*, *Lpl*, and *Smoc2*, known markers of quiescent/steady-state fibroblasts (Figure 4C through 4E; Figure S6C).^{8,20,21} The CF4 population was enriched in genes associated with actin cytoskeleton organization, whereas CF5 expressed genes were related to activated fibroblasts and ossification, including *Cilp*, *Comp*, and *Postn* (Figure 4C through 4E).¹⁴ The CF6 cluster expressed *Wif1*, a heart valve-associated fibroblast marker (previously designated F-Wnt-X) (Figure 4E).^{8,9,22} Although CF1 and CF3 ratios were mildly altered in Ctrl-HFpEF mice compared with those in Ctrl-chow mice, we did not detect a significant difference between Ctrl-HFpEF and TTg-HFpEF mice (Figure 4B; Figure S6A). Moreover, the profibrotic CF5 ratio, which greatly increased after MI,¹⁴ did not change among the 3 groups, suggesting that changes in the CF state did not contribute substantially to fibrosis in HFpEF.

We then analyzed differential gene expression by comparing each CF subtype in Ctrl-chow, Ctrl-HFpEF, and TTg-HFpEF mice to characterize the heterogenic response of CF clusters in HFpEF. After clustering significantly upregulated genes in Ctrl-HFpEF mice when compared with those in Ctrl-chow mice, we performed

Gene Ontology analysis based on the distinct gene expression per CF subtype and treatment (Figure 4F). Genes in cluster 2 were upregulated in CF1 to 3 in Ctrl-HFpEF mice and associated with ECM organizations, integrin cell surface interactions, supramolecular fiber organization, and TGF β (transforming growth factor β) receptor signaling regulation. Genes in cluster 1 were primarily upregulated in CF4 in Ctrl-HFpEF mice and functionally associated with actin filament-based processes, supramolecular fiber organization, and ECM organization, suggesting that these 2 clusters shared common features related to ECM organization and fibrosis. As shown by heatmap data, upregulated fibrotic genes in clusters 1 and 2, including *Loxl2*, *Fn1*, *Fbn1*, *Col1a1*, *Sparc*, *Col3a1*, and *Col5a3*, were primarily suppressed in TTg-HFpEF mice, suggesting a general antifibrotic effect associated with cardiac reprogramming across CF1 to 4 populations (Figure 4F). Cluster 4 genes, related to ossification, positive regulation of TGF β production, and ECM organization, were upregulated in the profibrotic CF5 population in Ctrl-HFpEF mice but suppressed in TTg-HFpEF mice. Conversely, genes in cluster 3 (related to cell death and stress response) were upregulated in CF3 and CF6 in Ctrl-HFpEF mice but were unaltered in TTg-HFpEF mice.

Next, we analyzed ECM scores that contain mRNA expression of all known ECM collagens, glycoproteins, and proteoglycans to quantitatively evaluate ECM gene expression in each CF cluster.⁶ The ECM scores were largely similar among the CF clusters, albeit slightly higher in CF5, and upregulated in Ctrl-HFpEF mice compared with Ctrl-chow mice in all CF clusters except CF6, whereas they were downregulated in TTg-HFpEF mice (Figure 4G). These results suggest that fibrotic profiles were diffusely upregulated in multiple CF clusters in HFpEF, which differed from the unique myofibrotic CF state transition detected after MI. Genes related to “response to stress” and “cell death” enriched in CF3 remained upregulated in TTg-HFpEF mice, which may be attributed to continuous HFD and L-NAME administration.

Consistent with the global changes in fibrotic profiles in HFpEF CFs, heatmap and gene expression analyses of CFs in Ctrl-chow, Ctrl-HFpEF, and TTg-HFpEF mice revealed that ECM, profibrotic genes, integrins, and TGF β /I16-related genes were all upregulated in Ctrl-HFpEF mice compared with those in Ctrl-chow mice, whereas they were suppressed in TTg-HFpEF mice (Figure 4H and 4I). Thus, profibrotic transcriptional changes induced in multiple CF clusters may be the primary contributors to fibrosis in HFpEF, which can be reversed with cardiac reprogramming.

CF Clusters Differentially Contributed to Interstitial and Perivascular Fibrosis in HFpEF

scRNA-seq analyses revealed the transcriptional profile of each CF cluster in HFpEF but did not provide spatial

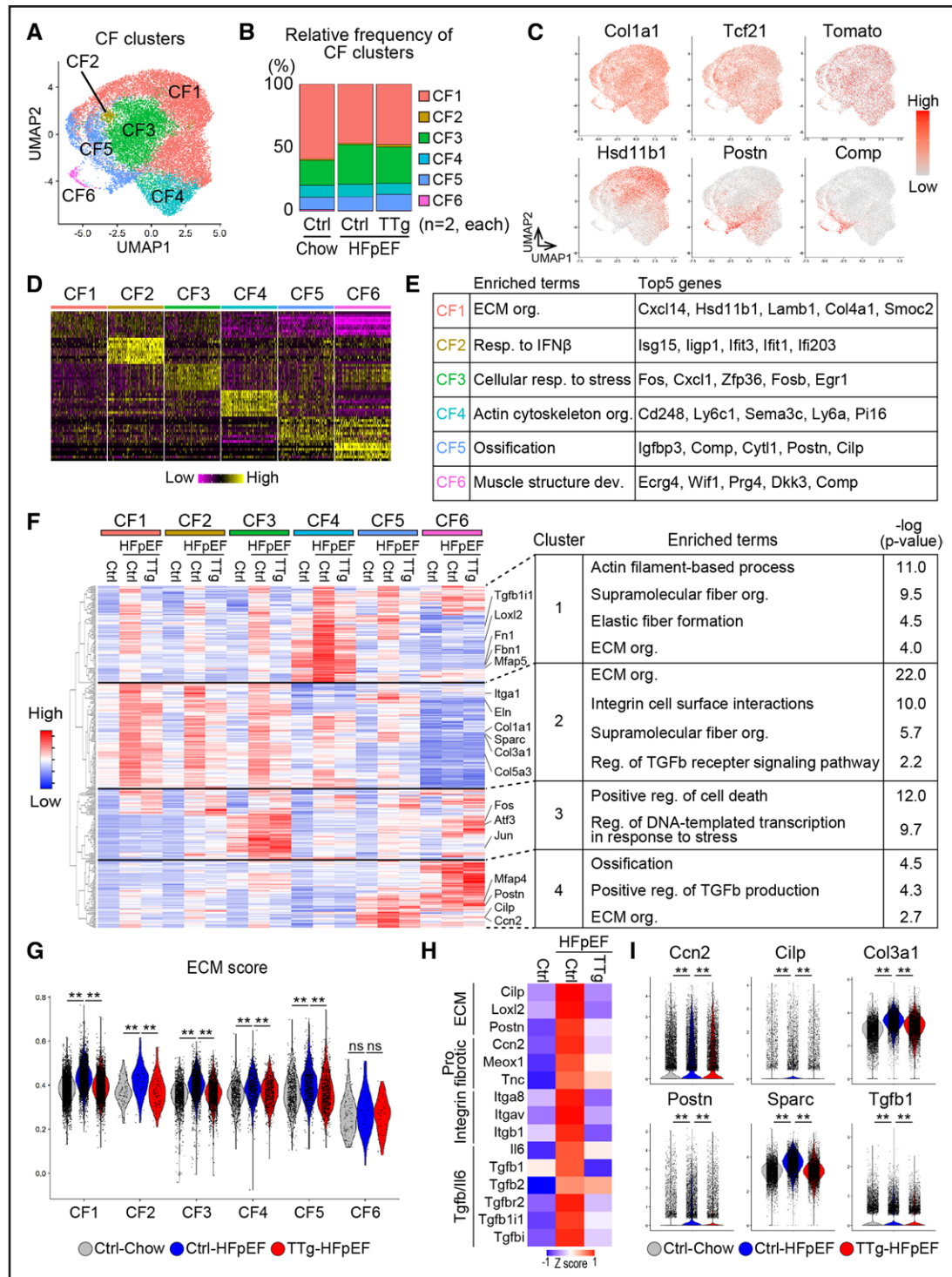


Figure 4. Cardiac reprogramming suppresses the profibrotic transcriptional program in multiple cardiac fibroblast clusters in HFpEF.

A, UMAP embedding 24 773 cardiac fibroblasts (CFs) from Ctrl-chow, Ctrl-HFpEF, and TTg-HFpEF mice. Six clusters (CF1–6) were identified. **B**, Bar plot of the percentage of CF cluster contributions in each group. **C**, Expression of select CF-related genes and Tomato as visualized on UMAP plots. **D**, Heatmap showing the top 10 marker gene expression per cluster in the scRNA-seq data. **E**, Selected representative GO terms and top 5 marker genes in each CF cluster. **F**, Hierarchical clustering analysis of differentially expressed genes analyzed by cluster and sample with selected representative significant enriched terms. **G**, Violin plot of extracellular matrix (ECM) scores per group and CF cluster. **H**, Heatmap of disease-related gene expressions in each group. **I**, Violin plots showing expression of ECM-related and profibrotic genes (*Ccn2*, *Cilp*, *Col3a1*, *Postn*, *Sparc*, and *Tgfb1*) in the CF population per group. ** $P < 0.01$ vs the relevant control using the Kruskal-Wallis with Dunn post hoc test. ns, Not significant. GO indicates Gene Ontology; HFpEF, heart failure with preserved ejection fraction; and scRNA-seq, single-cell RNA sequencing.

information. Therefore, we performed spatial transcriptomics to determine the localization and function of each CF cluster inducing interstitial and perivascular fibrosis in HFpEF. Spatial transcriptomic analysis of Ctrl-chow, Ctrl-HFpEF, and TTg-HFpEF mouse hearts revealed that HFpEF induced nonuniform distribution of fibrosis-related gene expression. The expression of *Col3a1* and *Sparc* expression enriched in CF1 to 4 was diffusely upregulated in the ventricles of the Ctrl-HFpEF mouse compared with those of the Ctrl-chow mouse (Figure 5A), whereas *Postn* and *Ccn2* enriched in the profibrotic CF5 cluster were focally upregulated in the Ctrl-HFpEF mouse ventricles (Figure 5B). To investigate the distribution and gene expression in each CF cluster in myocardial tissues, we combined spatial transcriptomic and scRNA-seq datasets by projecting marker gene expression of each CF subtype from scRNA-seq onto spatial transcriptomic data (Figure 5C). The spatial feature plot revealed that CF1 and CF3 marker gene scores were diffusely increased in the ventricles of the Ctrl-HFpEF mouse compared with those of the Ctrl-chow mouse, suggesting these CF clusters may predominantly contribute to diffuse interstitial fibrosis (Figure 5D). Conversely, CF5 and CF6 marker gene scores were locally upregulated in Ctrl-HFpEF mice, whereas CF4 scores were both locally and diffusely increased in HFpEF ventricles (Figure 5D). Intriguingly, Sirius red staining revealed that spots of locally elevated CF4 to 6 marker gene expression in Ctrl-HFpEF mice corresponded to perivascular fibrosis, although this type of fibrosis was not observed in Ctrl-chow and TTg-HFpEF (Figure 5E; Figure S7A and S7B). These results suggest that locally activated CF populations may contribute to perivascular fibrosis in the HFpEF heart. Consistently, immunohistochemistry revealed that *Postn*, a marker of activated CFs, was strongly expressed in the perivascular area along with Tomato⁺ CFs in Ctrl-HFpEF mice and was significantly reduced in TTg-HFpEF mice (Figure 5F; Figure S7C). Thus, although the results are a qualitative comparison of individual, representative animals for each group, we found that distinct CF clusters can differentially contribute to interstitial and perivascular cardiac fibrosis in HFpEF.

Gata4 Overexpression in CFs Improved Cardiac Fibrosis and Diastolic Dysfunction in HFpEF

Overexpression of 4 cardiac reprogramming factors, MGTH, in CFs, reduced fibrosis and improved diastolic dysfunction in HFpEF. Because myocardial contraction is preserved in HFpEF, cardiomyocyte regeneration may be unnecessary for improved cardiac performance in HFpEF. To determine whether overexpression of a single reprogramming factor could sufficiently improve cardiac function in HFpEF, we generated new transgenic mice expressing the individual factors, *Gata4*, *Mef2c*, *Tbx5*, and *Hand2* (designated SF-G, M, T, and H), under the control

of the CAG promoter and flox-stop allele by knock-in to the *Rosa26* locus (Figure 6A). First, to screen factors that could induce antifibrotic effects in vitro, we obtained mouse embryonic fibroblasts from SF-G, M, T, and H and MGTH2A mice, transduced retroviral pMX-Cre, and analyzed gene expression after 1 week (Figure 6A and 6B). Reverse-transcription quantitative polymerase chain reaction revealed that *Gata4*, *Mef2c*, *Tbx5*, and *Hand2* were successfully expressed in SF-G, M, T, H, and MGTH2A mouse embryonic fibroblasts with specific gene expression in each group. Profibrotic genes were consistently downregulated in SF-G and MGTH2A but not in SF-M, T, and H mouse embryonic fibroblasts (Figure 6B). Fluorescence-activated cell sorting analysis revealed that overexpression of MGTH, but not individual factors, induced cTnT (cardiac troponin T) in mouse embryonic fibroblasts and adult mouse CFs (Figure 6C; Figure S8A). Thus, among the 4 factors, only *Gata4* overexpression could induce antifibrotic effects without generating new iCMs in vitro.

We then generated tamoxifen-inducible double transgenic mice overexpressing G, M, and MGTH in CFs by crossing *Tcf21*^{Cre} and SF-G, M, and MGTH2A mice (Figure 6D). To induce HFpEF, control (Ctrl and *Tcf21*^{Cre}) and *Tcf21*^{Cre}/SF-G, M, and MGTH2A mice were subjected to HFD feeding and administered L-NAME. After 5 weeks of HFpEF induction, all groups received tamoxifen for 5 consecutive days. Hearts were harvested at 10 weeks when cardiac fibrosis was established (Figure S3B). Body weight and blood pressure increased in all 4 groups receiving HFD+L-NAME compared with those in the Ctrl-chow group (Figure S8B). Echocardiography showed that LV wall thickness was improved in SF-G-HFpEF and MGTH2A-HFpEF, whereas cardiac contraction and LV inner diameter were unaltered (Figure S8C and S8D). Elevated E/A and E/E' observed in HFpEF were significantly suppressed in SF-G-HFpEF and MGTH2A-HFpEF mice but not in SF-M-HFpEF mice (Figure 6E). Cardiac function was preserved in the SF-G-chow mice when compared with that in Ctrl-chow mice, suggesting *Gata4* expression alone did not induce any phenotype in mice (Figure S8E). The cardiac catheter indices (LV end-diastolic pressure and end-diastolic pressure-volume relationship) and treadmill tests also revealed significant improvements in SF-G-HFpEF and MGTH2A-HFpEF mice compared with Ctrl-HFpEF and SF-M-HFpEF mice (Figures 6F and 6G). Fibrosis was strongly reduced in SF-G-HFpEF and MGTH2A-HFpEF mice but not in SF-M-HFpEF mice (Figure 6H). Consistent with these results, fibrosis-related genes and a fetal gene program (*Nppb*) were significantly downregulated in SF-G-HFpEF and MGTH2A-HFpEF hearts compared with those in Ctrl-HFpEF and SF-M-HFpEF hearts (Figure S8F).

We next generated *Tcf21*^{Cre}/Tomato/SF-G mice by crossing *Tcf21*^{Cre}/SF-G mice with Tomato mice for histological analysis. Consistent with the antifibrotic effect

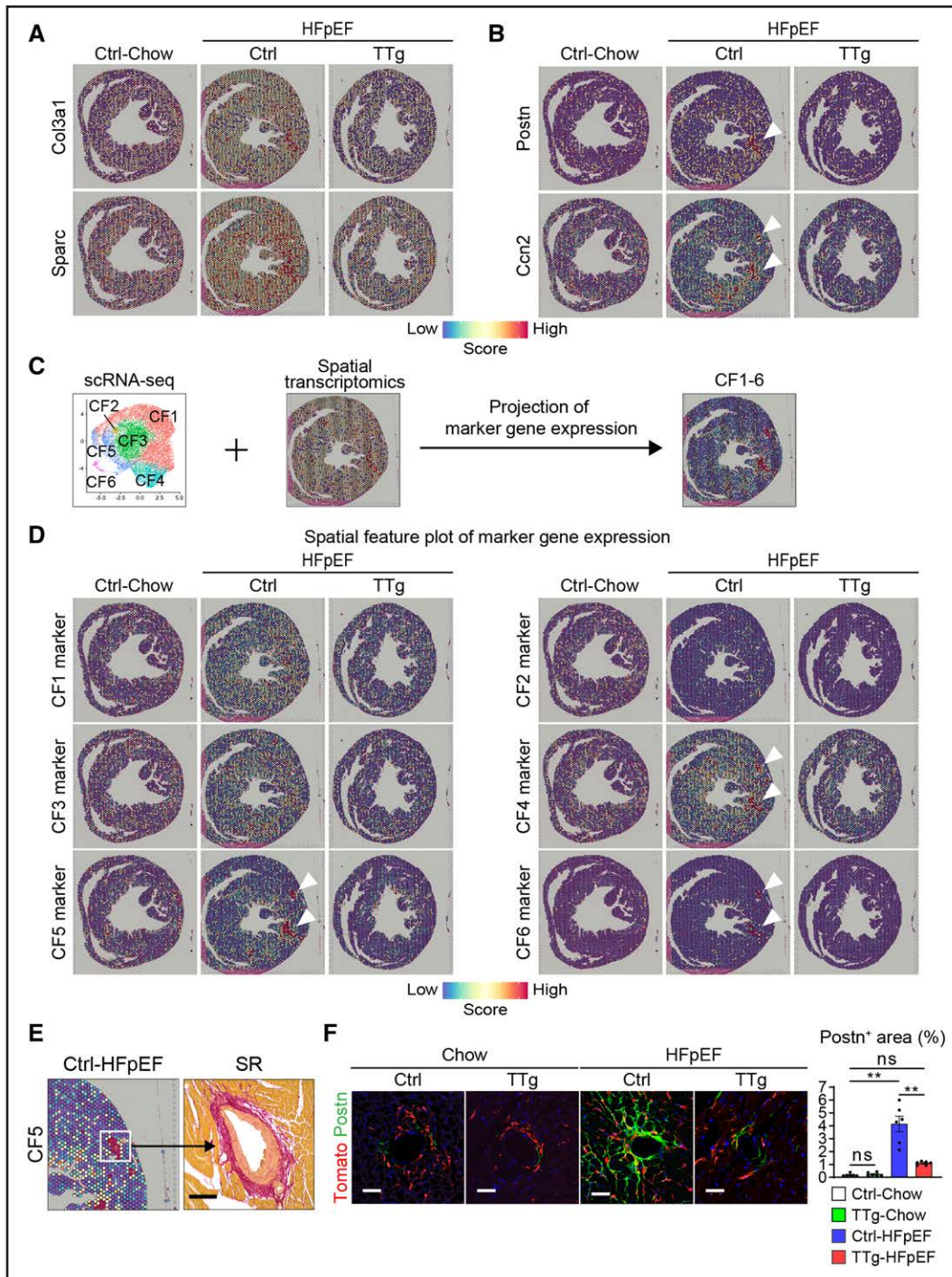


Figure 5. Spatial transcriptomics demonstrates the contribution of each cardiac fibroblast cluster to interstitial and perivascular fibrosis.

A and **B**, Spatially resolved gene expression of fibrosis-related genes. White arrowheads indicate the focally upregulated regions in Ctrl-HFpEF (**B**). **C**, Schematic diagram of combinational analyses of scRNA-seq and spatial transcriptomics. **D**, Spatial feature plots of the average score of the top 30 marker gene expression in each cardiac fibroblast (CF) cluster. White arrowheads indicate focally upregulated CF4–6 marker gene expression spots in Ctrl-HFpEF mice. **E**, Upregulated spot of CF5 marker gene expression and Sirius red (SR) staining in Ctrl-HFpEF mice. SR staining of serial sections for spatial transcriptomics shows the colocalization of CF5 marker gene expression and perivascular fibrosis. **F**, Immunohistochemistry of Tomato, Postn, and DAPI in Ctrl-chow, TTg-chow, Ctrl-HFpEF, and TTg-HFpEF mouse hearts at 15 weeks. Quantitative analysis for the Postn⁺ areas is shown (n=6 independent biological replicates). All data are presented as the mean±SEM. ***P*<0.01 vs the relevant control using 1-way ANOVA followed by Tukey multicomparisons test. Scale bars represent 100 μm (**E**) and 50 μm (**F**). HFpEF indicates heart failure with preserved ejection fraction; scRNA-seq, single-cell RNA sequencing; and SEM, standard error of the mean.

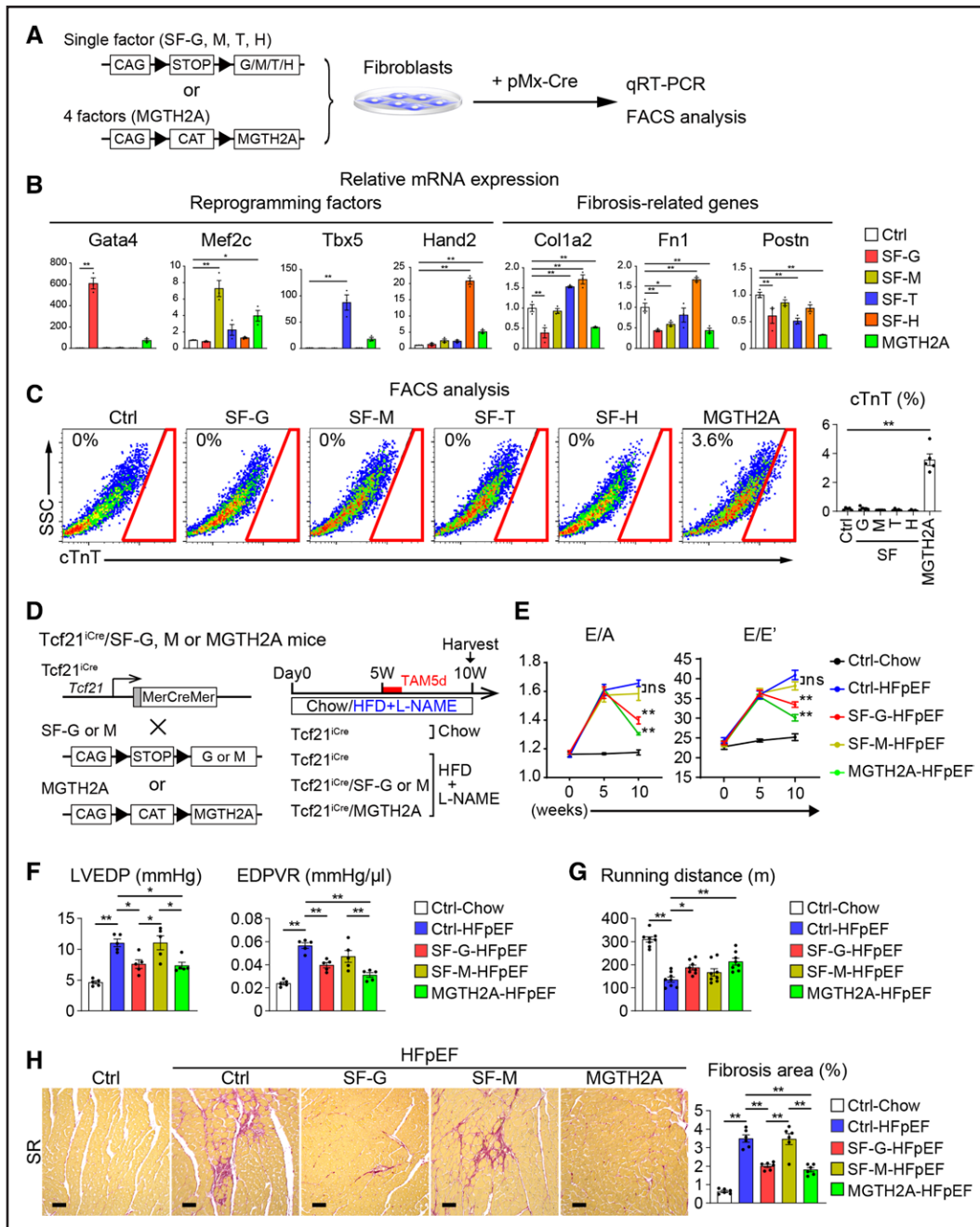


Figure 6. Gata4 overexpression can improve cardiac function and fibrosis in HFpEF.

A, Schematic of pMX-Cre transduction in mouse fibroblasts to induce the expression of a single factor (SF-G, M, T, H) through Cre-mediated recombination. **B**, Relative mRNA expression of reprogramming factors (*Gata4*, *Mef2c*, *Tbx5*, and *Hand2*) and fibrosis-related genes (*Col1a2*, *Fn1*, and *Postn*) 1 week after transduction (n=3 independent biological replicates). **C**, FACS analysis for cTnT (cardiac troponin T) expression in mouse embryonic fibroblasts transduced with pMX-Cre after 1 week. Quantitative data are shown (n=5 independent biological replicates). **D**, Strategy for Gata4, Mef2c, or MGTH2A overexpression using double transgenic mice generated by crossing *Tcf21*^{Cre} mice with SF mice (SF-G, or M) or MGTH2A mice. TAM administration induces Gata4, Mef2c, or MGTH2A expression in *Tcf21*-expressing resident CFs in vivo. **Right**, Experimental scheme of TAM and HFD+L-NAME treatment. Hearts were harvested 10 weeks after treatment initiation (5 weeks after TAM administration). **E**, E/A ratio and E/E' ratio were serially quantified in the indicated groups (n=8 independent biological replicates) using echocardiography. **F**, Quantitative analyses of LVEDP and EDPVR (n=5 independent biological replicates). **G**, Running distance during treadmill test (n=8 independent biological replicates). **H**, Representative images of Sirius red (SR) staining of the left ventricle of the fibrotic area (n=6 independent biological replicates) is shown. All data are presented as the mean±SEM. **P*<0.05, ***P*<0.01 vs the relevant control using 1-way ANOVA followed by Dunnett multicomparisons test (**B** and **C**) and 1-way ANOVA followed by Tukey multicomparisons test (**F** through **H**). ***P*<0.01 vs Ctrl-HFpEF using 2-way ANOVA followed by Tukey multicomparisons test (**E**). ns, Not significant. Scale bars=50 μm. EDPVR indicates end-diastolic pressure-volume relationship; HFpEF, heart failure with preserved ejection fraction; LVEDP, left ventricular end-diastolic pressure; SEM, standard error of the mean; and TAM, tamoxifen.

of Gata4 overexpression, BrdU⁺ proliferative CFs were reduced in SF-G-HFpEF mice compared with those in Ctrl-HFpEF mice, whereas TUNEL⁺ apoptotic CFs were unchanged (Figure S9A and S9B). POSTN was expressed in the perivascular area along with Tomato⁺ CFs in the Ctrl-HFpEF, whereas this expression was significantly reduced in SF-G-HFpEF, although the presence of Tomato⁺ CFs was detected (Figure S9C and S9D). Capillary density, reduced in Ctrl-HFpEF mice, was recovered in SF-G-HFpEF mice without altering large-vessel diameter (Figure S9E through S9H). Thus, overexpression of a single factor, Gata4, could sufficiently reduce fibrosis and improve HFpEF.

Gata4 Inhibited CF Activation by Suppressing *Meox1*

Subsequently, we investigated the molecular mechanism underlying Gata4-induced antifibrotic effects in HFpEF. *MEOX1* acts as a major regulator of CF activation, and antifibrotic effects of in vivo cardiac reprogramming through MGTH overexpression in chronic MI are mediated through suppression of *Meox1*; however, it remains unknown whether overexpression of Gata4 alone can suppress *Meox1* to reduce fibrosis. If so, the mechanism through which Gata4 regulates *Meox1* expression in CFs needs to be elucidated.⁷ Reverse-transcription quantitative polymerase chain reaction results revealed that *Meox1* was significantly upregulated in HFpEF ventricles, whereas this expression was downregulated not only in MGTH2A-HFpEF but also in SF-G-HFpEF, suggesting Gata4 overexpression alone suppressed *Meox1* in HFpEF (Figure 7A). In vitro experiments revealed that small interfering RNA (siMeox1)-mediated suppression of *Meox1* reduced the mRNA expression of *Acta2* (alpha-smooth muscle actin [α SMA]), a marker of activated fibroblasts, in adult mouse CFs treated with TGF β (Figure 7B and 7C). Gata4 overexpression with Sendai virus vectors (SeV-Gata4) also suppressed *Meox1* and *Acta2* expression in mouse CFs. The addition of siMeox1 to SeV-Gata4 did not further downregulate *Meox1* and *Acta2* expression (Figure 7C). Moreover, immunocytochemistry revealed that siMeox1 and SeV-Gata4 reduced α SMA expression in mouse CFs treated with TGF β , and that the addition of siMeox1 to SeV-Gata4 did not further reduce α SMA, suggesting that Gata4 suppressed CF activation mainly through *Meox1* inhibition (Figure 7D). GATA4 was found to directly repress noncardiac gene programs in the developing heart by recruiting a chromatin remodeling complex repressing gene expression.²³ To investigate whether Gata4 can directly suppress *Meox1* expression, we analyzed Gata4 binding sites and H3K27ac expression, an active histone mark, at the enhancer regions of the *Meox1* gene using publicly available chromatin immunoprecipitation followed by sequencing data of control and MGTH-transduced fibroblasts.²⁴ Gata4 was bound directly to the

enhancer regions of *Meox1*, where H3K27ac peaks were significantly suppressed in MGTH-transduced fibroblasts (Figure S10A). These results suggest that Gata4 overexpression can directly suppress *Meox1* through epigenetic silencing to inhibit the fibroblast program.

We next analyzed whether fibroblast activation and repression may affect cardiomyocyte function. To determine the paracrine effects of CFs on cardiomyocytes, we cultured CFs treated with or without TGF β and collected conditioned media after 3 days. Then, neonatal rat cardiomyocytes were treated with collected conditioned media for 2 days (Figure S10B). Compared with Ctrl CF-conditioned media, TGF β -treated CF-conditioned media significantly induced cardiomyocyte hypertrophy. Conditioned media from CFs treated with TGF β and SeV-Gata4 markedly suppressed cardiomyocyte hypertrophy, suggesting CFs can affect cardiomyocyte function in a paracrine manner (Figure S10C).

Finally, we determined whether Gata4 overexpression also induced antifibrotic effects in TGF β -treated human CFs (Figure 7E). Gata4 overexpression significantly downregulated the expression of profibrotic and *TGFB1*-related genes, including *ACTA2*, *Col1A1*, *POSTN*, *TGFB1*, *CTGF*, and *MEOX1*, in human CFs. Immunocytochemistry showed that SeV-Gata4 reduced α SMA-positive CFs, suggesting that Gata4 also induced antifibrotic effects in human CFs (Figure 7F and 7G).

DISCUSSION

HFpEF is a major health problem and a leading cause of mortality worldwide. Although cardiac fibrosis may be a promising target to treat HFpEF, the mechanisms of fibrosis in HFpEF remain unclear, and no effective therapies targeting fibrosis have been established.²⁵ Here, we demonstrated that MGTH overexpression in resident CFs ameliorated pathological changes and improved diastolic dysfunction in HFpEF. scRNA-seq and spatial transcriptomics revealed that profibrotic transcriptional changes were induced in multiple CF clusters, leading to diffuse interstitial fibrosis, whereas distinct CF clusters contributed to perivascular fibrosis in HFpEF. These fibrotic changes can be reversed with cardiac reprogramming. Among 4 cardiac reprogramming factors, overexpression of Gata4 could sufficiently improve cardiac function and reduce fibrosis in HFpEF.

HFpEF pathogenesis involves multiple pathophysiological changes, such as cardiac hypertrophy, fibrosis, inflammation, metabolic stress, and capillary loss.^{1,12} Cardiac fibrosis can be an underlying cause and result of these changes, thereby creating a feed-forward loop of disease progression.^{4,13} CFs interact with multiple cell types, including cardiomyocytes, ECs, immune cells, and smooth muscle cells, and our CellChat analysis revealed the interactions between CFs and ECs through VEGF-VEGFR and Angptl4-Cdh5 signaling.²⁶ Gata4 expression

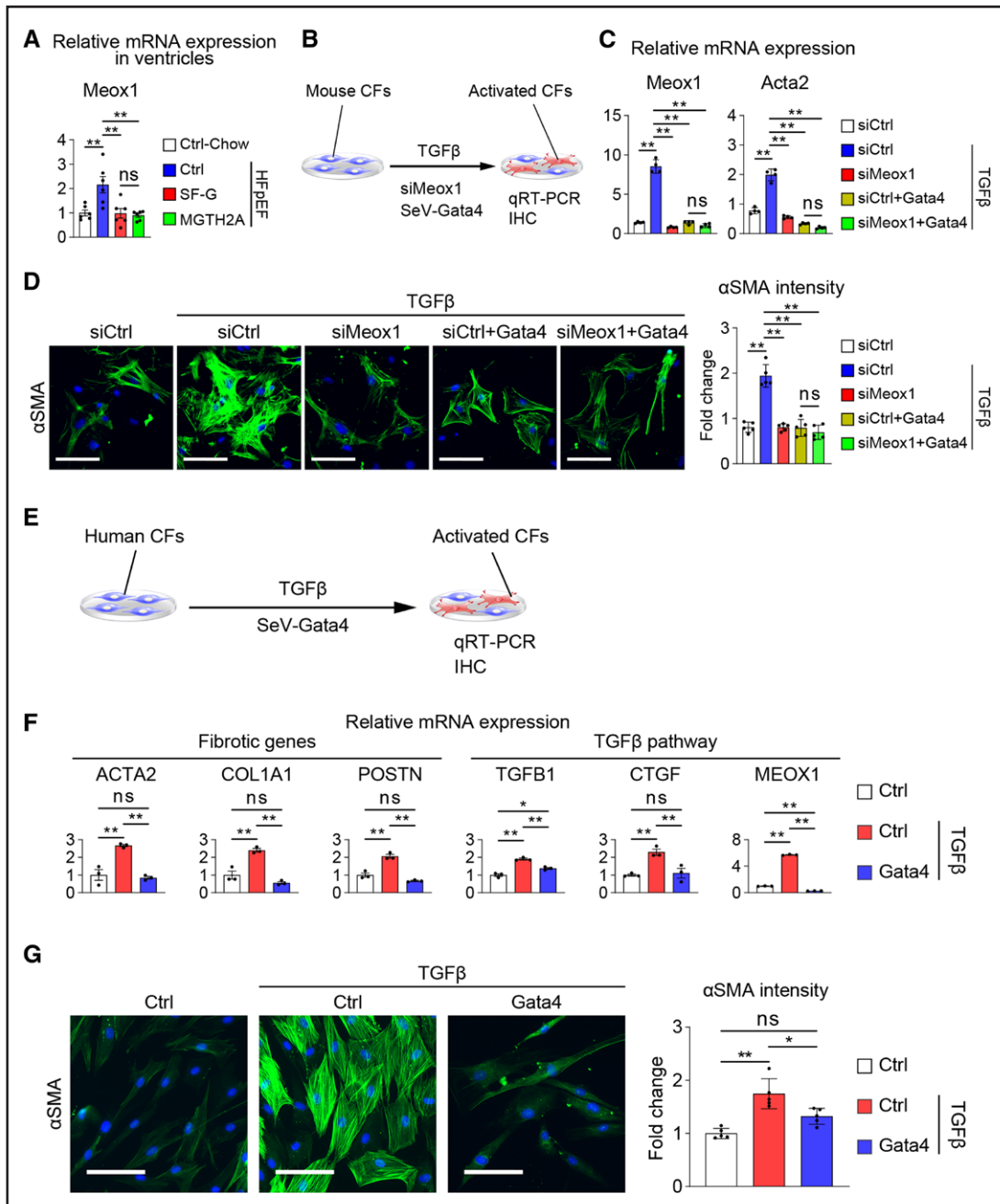


Figure 7. Gata4 overexpression suppresses cardiac fibroblast activation through Meox1 inhibition.

A, Relative mRNA expression of *Meox1* in mouse ventricles in the indicated groups ($n=6$ independent biological replicates). **B**, Schematic representation of the protocol for Meox1 knockdown (siMeox1) and Gata4 overexpression (SeV-Gata4) in adult mouse cardiac fibroblasts (CFs) treated with TGF- β . RT-qPCR (**C**) and immunocytochemistry (**D**) were performed after 3 days. **C**, Relative mRNA expression of *Meox1* and *Acta2* in the indicated groups ($n=4$ independent biological replicates). **D**, Immunocytochemistry for α SMA and DAPI. Both Gata4 transduction and Meox1 knockdown reduce the formation of α SMA-positive stress fibers in TGF β -treated CFs after 3 days. Quantitative analysis of fluorescence intensity normalized by cell number is shown ($n=5$ independent biological replicates). **E**, Schematic representation of the protocol for Gata4 overexpression in human CFs. CFs were infected with SeV-Gata4 and treated with TGF- β 1. RT-qPCR (**F**) and immunohistochemistry (**G**) were analyzed at 3 days after SeV-Gata4 transduction. **F**, Relative mRNA expression of fibrosis- and TGF β pathway-related genes was measured using RT-qPCR ($n=3$ independent biological replicates). **G**, Immunofluorescence staining of α SMA and DAPI in human CFs. Quantitative analysis of fluorescence intensity normalized by cell number is shown ($n=5$ independent biological replicates). All data are presented as the mean \pm SEM. * $P<0.05$, ** $P<0.01$ vs the relevant control by 1-way ANOVA followed by Tukey multicomparisons test. ns, Not significant. Scale bars=100 μ m. α SMA indicates alpha-smooth muscle actin; RT-qPCR, reverse-transcription quantitative polymerase chain reaction; SEM, standard error of the mean; and TGF β , transforming growth factor β .

in cardiomyocytes has been shown to induce angiogenesis through VEGF expression in the mouse heart,²⁷ suggesting such proangiogenic signaling may increase the capillary density in MGTH- and SF-G-HFpEF mice. However, because our cell isolation protocol selected viable cells, cell types sensitive to cell death may not be detected in sufficient numbers in scRNA-seq analysis, obscuring the exact cell composition. Despite this limitation, it is conceivable that the relative changes in cell composition and cell-cell interactions between different samples were not affected, given that the cells were treated using the same protocol.²⁸

The fibrotic area was increased to approximately 3% in HFpEF mouse ventricles, which was reduced to approximately 1.5% by MGTH or Gata4 expression in CFs (Figures 2H and 6H). Furthermore, the amount of fibrosis was well-correlated with diastolic dysfunction in HFpEF mice, although the level of fibrosis in HFpEF was generally modest. Pathophysiologically relevant cardiac fibrosis below the limit of detection of standard histochemical staining may also contribute to diastolic dysfunction in HFpEF, as reported recently.²⁹ Further studies using mass spectrometry and atomic force microscopy are required to evaluate the effects of such hidden fibrosis.²⁹ Alternatively, as increased myocardial stiffness in patients with HFpEF is determined by ECM fibrillar collagen and cardiomyocyte structures,⁴ fibrosis, cardiomyocyte hypertrophy, and cardiomyocyte stiffness caused by titin dysregulation may contribute to diastolic dysfunction. Cardiomyocyte hypertrophy and myocardial relaxation were improved in MGTH- and SF-G-HFpEF mice. Reportedly, activation of TGF β signaling induces not only fibrosis but also cardiac hypertrophy, whereas TGF β suppression ameliorates these changes in mice.^{30–33} Consistently, we found that cardiomyocyte hypertrophy was induced in TGF β -treated CFs in a paracrine manner, whereas Gata4 overexpression in CFs suppressed CF activation and cardiomyocyte hypertrophy, suggesting that CF-cardiomyocyte interaction may also contribute to the diastolic dysfunction in HFpEF.

After MI, the formation of extensive fibrosis (scar tissue) is induced by the cell state transition of quiescent CFs to myofibroblastic CFs, which produce ECM and replace myocardial loss.^{8,10} Cardiac reprogramming can reverse profibrotic CF transition and thereby reduce fibrosis in MI.¹⁴ In contrast, interstitial and perivascular fibrosis is slowly generated in HFpEF in response to chronic stress. Based on our scRNA-seq results, there were no significant alterations in relative ratios of CF clusters in HFpEF or after cardiac reprogramming. Expression of multiple ECM genes and ECM scores was upregulated in multiple CF populations in HFpEF, which was reversed with cardiac reprogramming. Accordingly, our results indicate substantial diversity in the mode of CF activation and fibrosis depending on the cardiac disorders, such as MI and HFpEF. CF cell state transition likely accounts for

replacement fibrosis to prevent ventricular wall rupture after MI, whereas profibrotic transcriptional changes in multiple CF clusters mainly contribute to interstitial/perivascular fibrosis in HFpEF. However, the possibility that CF cell state transition occurs in HFpEF at different time points or below the detection limit of our scRNA-seq analysis cannot be excluded.

Combining scRNA-seq and spatial transcriptomics revealed additional mechanisms for generating interstitial and perivascular fibrosis in HFpEF. The spatial feature plots of gene expression scores in multiple CF clusters were diffusely upregulated in HFpEF ventricles, suggesting that these clusters primarily contribute to interstitial fibrosis. Conversely, the expression of POSTN-expressing profibrotic CF populations was focally upregulated in HFpEF hearts, corresponding to perivascular fibrosis. These profibrotic changes were reversed by overexpression of MGTH and Gata4 in CFs. Mechanistically, we found that Gata4 may directly bind to the enhancer regions of Meox1, a key regulator of fibrosis, to repress fibrosis. To the best of our knowledge, this is the first study to demonstrate that distinct CF clusters differentially contribute to interstitial and perivascular fibrosis in HFpEF.

This study has some limitations. First, only male mice were used, and the effects in female mice were not analyzed.^{18,34} Second, the effects of cardiac reprogramming and regeneration in HFpEF remained unclear; however, the number of iCM generations was limited with cardiac reprogramming, and only Gata4 overexpression improved HFpEF without generating iCMs, suggesting that improved HFpEF was mainly mediated by antifibrotic effects in this model.

Overall, cardiac reprogramming reduces fibrosis in HFpEF ventricles, improving diastolic dysfunction and cardiac performance. Gata4 overexpression also reduces fibrosis and improves HFpEF. Consistently, Gata4 overexpression has ameliorated fibrosis after MI and in the liver.^{35,36} For future clinical application of in vivo reprogramming, overexpression of only one factor, Gata4, would be technically simpler than expressing all 4 MGTH factors simultaneously with high efficiency. Moreover, CF state modification mediated through Gata4 overexpression may be a safer strategy than CF ablation using antifibrotic chimeric antigen receptor (CAR) T cells, which may induce inflammation in the heart.^{11,37} Although the development of CF-specific vectors may be critical for clinical application,³⁸ in vivo gene transfer of Gata4 may be a promising approach for reducing fibrosis and treating HFpEF.

ARTICLE INFORMATION

Received October 6, 2023; accepted October 24, 2024.

Affiliations

Department of Cardiology (Y.Y., K.N., S.H., Y.A., T.A., R.F.), Department of Respiratory Medicine (T.A.), Department of Hematology (M.S.-Y., S.C.), Department of

Cardiovascular Surgery (H.K., H.S., Y.H.), Institute of Medicine, Division of Regenerative Medicine, Transborder Medical Research Center (R.F.), University of Tsukuba, Japan. Department of Cardiology, Keio University School of Medicine (T.S., M.N., T.M., M.I.), Department of Molecular Biology (C.T., K.M.), Tokyo, Japan. Department of Computational Biology and Medical Sciences, Graduate School of Frontier Sciences, University of Tokyo, Chiba, Japan (Y.K., M.O., M.S., Y.S.). Laboratory for Functional Non-coding Genomics, RIKEN Center for Integrative Medical Sciences, Yokohama, Japan (Y.W.I.).

Acknowledgments

The authors are grateful to S. Mizuno for providing pROSA-CAG-LSL-pA. They are also grateful to the current and former members of the Ieda Laboratory and T. Yamamoto for their support and discussions and to the Animal Research Facility (Tsukuba University) staff for animal care. We thank the Life Science Data Research Center for the sequencing and analysis. The supercomputing resources were provided by the Human Genome Center, the Institute of Medical Science, University of Tokyo (<http://sc.hgc.jp/shirokane.html>). Y.Y., T.S., and M.I. designed the experiments. Y.Y. generated transgenic mice. Y.Y., S.H., and T.S. performed the in vitro experiments. Y.Y., K.N., Y.A., T.A., R.F., M.N., and T.M. performed the in vivo experiments. Y.Y., T.S., Y.K., M.O., M.S., Y.S., M.S.Y., S.C., T.C., K.M., and Y.W.I. performed transcriptomics and analyzed the data. Y.Y., T.S., H.K., H.S., and Y.H. performed experiments on human cardiac fibroblasts. Y.Y., T.S., and M.I. wrote the article.

Sources of Funding

This work was supported by research grants from the Research Center Network for Realization of Regenerative Medicine (JP20bm0704030 and JP22bm1123012), the Japan Agency for Medical Research and Development, the Japan Foundation for Applied Enzymology, MSD Life Science Foundation, the Mitsubishi Foundation, the Japan Society for the Promotion of Science (21K08072, 21K19471, 22H03065, 23K24326, and 24K02850), and the Takeda Science Foundation.

Disclosures

None.

Supplemental Material

Supplemental Methods

Figure S1–S10

Tables S1–S3

References 39–50

REFERENCES

- Mishra S, Kass DA. Cellular and molecular pathobiology of heart failure with preserved ejection fraction. *Nat Rev Cardiol*. 2021;18:400–423. doi: 10.1038/s41569-020-00480-6
- Schiattarella GG, Alcaide P, Condorelli G, Gillette TG, Heymans S, Jones EAV, Kallikourdis M, Lichtman A, Marelli-Berg F, Shah S, et al. Immuno-metabolic mechanisms of heart failure with preserved ejection fraction. *Nat Cardiovasc Res*. 2022;1:211–222. doi: 10.1038/s44161-022-00032-w
- Hahn VS, Yanek LR, Vaishnav J, Ying W, Vaidya D, Lee YZJ, Riley SJ, Subramanya V, Brown EE, Hopkins CD, et al. Endomyocardial biopsy characterization of heart failure with preserved ejection fraction and prevalence of cardiac amyloidosis. *JACC Heart Fail*. 2020;8:712–724. doi: 10.1016/j.jchf.2020.04.007
- Zile MR, Baicu CF, Ikonomidis JS, Stroud RE, Nietert PJ, Bradshaw AD, Slater R, Palmer BM, Van Buren P, Meyer M, et al. Myocardial stiffness in patients with heart failure and a preserved ejection fraction: contributions of collagen and titin. *Circulation*. 2015;131:1247–1259. doi: 10.1161/CIRCULATIONAHA.114.013215
- Pinto AR, Ilinykh A, Ivey MJ, Kuwabara JT, D'Antoni ML, Debuque R, Chandran A, Wang L, Arora K, Rosenthal NA, et al. Revisiting cardiac cellular composition. *Circ Res*. 2016;118:400–409. doi: 10.1161/CIRCRESAHA.115.307778
- Peisker F, Halder M, Nagai J, Ziegler S, Kaesler N, Hoeft K, Li R, Bindels EMJ, Kuppe C, Moellmann J, et al. Mapping the cardiac vascular niche in heart failure. *Nat Commun*. 2022;13:3027. doi: 10.1038/s41467-022-30682-0
- Alexanian M, Przytycki PF, Micheletti R, Padmanabhan A, Ye L, Travers JG, Gonzalez-Teran B, Silva AC, Duan Q, Ranade SS, et al. A transcriptional switch governs fibroblast activation in heart disease. *Nature*. 2021;595:438–443. doi: 10.1038/s41586-021-03674-1
- Forte E, Skelly DA, Chen M, Daigle S, Morelli KA, Hon O, Philip VM, Costa MW, Rosenthal NA, Furtado MB. Dynamic interstitial cell response during myocardial infarction predicts resilience to rupture in genetically diverse mice. *Clin Rep*. 2020;30:3149–3163.e6. doi: 10.1016/j.celrep.2020.02.008
- Farbehi N, Patrick R, Dorison A, Xaymardan M, Janbandhu V, Wystub-Lis K, Ho JW, Nordon RE, Harvey RP. Single-cell expression profiling reveals dynamic flux of cardiac stromal, vascular and immune cells in health and injury. *Elife*. 2019;8:e43882. doi: 10.7554/eLife.43882
- Fu X, Khalil H, Kanisicak O, Boyer JG, Vagnozzi RJ, Maliken BD, Sargent MA, Prasad V, Valiente-Alandi I, Blaxall BC, et al. Specialized fibroblast differentiated states underlie scar formation in the infarcted mouse heart. *J Clin Invest*. 2018;128:2127–2143. doi: 10.1172/JCI98215
- Kanisicak O, Khalil H, Ivey MJ, Karch J, Maliken BD, Correll RN, Brody MJ, Lin S-CJ, Aronow BJ, Tallquist MD, et al. Genetic lineage tracing defines myofibroblast origin and function in the injured heart. *Nat Commun*. 2016;7:12260. doi: 10.1038/ncomms12260
- Roh J, Hill JA, Singh A, Valero-Munoz M, Sam F. Heart failure with preserved ejection fraction: heterogeneous syndrome, diverse preclinical models. *Circ Res*. 2022;130:1906–1925. doi: 10.1161/CIRCRESAHA.122.320257
- Mohammed SF, Hussain S, Mirzoyev SA, Edwards WD, Maleszewski JJ, Redfield MM. Coronary microvascular rarefaction and myocardial fibrosis in heart failure with preserved ejection fraction. *Circulation*. 2015;131:550–559. doi: 10.1161/CIRCULATIONAHA.114.009625
- Tani H, Sadahiro T, Yamada Y, Isomi M, Yamakawa H, Fujita R, Abe Y, Akiyama T, Nakano K, Kuze Y, et al. Direct reprogramming improves cardiac function and reverses fibrosis in chronic myocardial infarction. *Circulation*. 2023;147:223–238. doi: 10.1161/CIRCULATIONAHA.121.058655
- Miyamoto K, Akiyama M, Tamura F, Isomi M, Yamakawa H, Sadahiro T, Muraoka N, Kojima H, Haginiwa S, Kurotsu S, et al. Direct in vivo reprogramming with Sendai virus vectors improves cardiac function after myocardial infarction. *Cell Stem Cell*. 2018;22:91–103.e5. doi: 10.1016/j.stem.2017.11.010
- Qian L, Huang Y, Spencer CI, Foley A, Vedantham V, Liu L, Conway SJ, Wu JD, Srivastava D. In vivo reprogramming of murine cardiac fibroblasts into induced cardiomyocytes. *Nature*. 2012;485:593–598. doi: 10.1038/nature11044
- Song K, Nam YJ, Luo X, Qi X, Tan W, Huang GN, Acharya A, Smith CL, Tallquist MD, Neilson EG, et al. Heart repair by reprogramming non-myocytes with cardiac transcription factors. *Nature*. 2012;485:599–604. doi: 10.1038/nature11139
- Schiattarella GG, Altamirano F, Tong D, French KM, Villalobos E, Kim SY, Luo X, Jiang N, May HI, Wang ZV, et al. Nitrosative stress drives heart failure with preserved ejection fraction. *Nature*. 2019;568:351–356. doi: 10.1038/s41586-019-1100-z
- Cuijpers I, Simmonds SJ, van Bilsen M, Czarnowska E, Gonzalez Miqueo A, Heymans S, Kuhn AR, Mulder P, Ratajska A, Jones EAV, et al. Microvascular and lymphatic dysfunction in HFpEF and its associated comorbidities. *Basic Res Cardiol*. 2020;115:39. doi: 10.1007/s00395-020-0798-y
- Buechler MB, Pradhan RN, Krishnamurthy AT, Cox C, Calviello AK, Wang AW, Yang YA, Tam L, Caothien R, Roose-Girma M, et al. Cross-tissue organization of the fibroblast lineage. *Nature*. 2021;593:575–579. doi: 10.1038/s41586-021-03549-5
- McLellan MA, Skelly DA, Dona MSI, Squiers GT, Farrugia GE, Gaynor TL, Cohen CD, Pandey R, Diep H, Vinh A, et al. High-resolution transcriptomic profiling of the heart during chronic stress reveals cellular drivers of cardiac fibrosis and hypertrophy. *Circulation*. 2020;142:1448–1463. doi: 10.1161/CIRCULATIONAHA.119.045115
- Muhl L, Genove G, Leptidis S, Liu J, He L, Mocci G, Sun Y, Gustafsson S, Buyandelger B, Chivukula IV, et al. Single-cell analysis uncovers fibroblast heterogeneity and criteria for fibroblast and mural cell identification and discrimination. *Nat Commun*. 2020;11:3953. doi: 10.1038/s41467-020-17740-1
- Robbe ZL, Shi W, Wasson LK, Scialdone AP, Wilczewski CM, Sheng X, Hepperla AJ, Akerberg BN, Pu WT, Cristea IM, et al. CHD4 is recruited by GATA4 and NKX2-5 to repress noncardiac gene programs in the developing heart. *Genes Dev*. 2022;36:468–482. doi: 10.1101/gad.349154.121
- Hashimoto H, Wang Z, Garry GA, Malladi VS, Botten GA, Ye W, Zhou H, Osterwalder M, Dickel DE, Visel A, et al. Cardiac reprogramming factors synergistically activate genome-wide cardiogenic stage-specific enhancers. *Cell Stem Cell*. 2019;25:69–86.e5. doi: 10.1016/j.stem.2019.03.022
- Sweeney M, Corden B, Cook SA. Targeting cardiac fibrosis in heart failure with preserved ejection fraction: mirage or miracle? *EMBO Mol Med*. 2020;12:e10865. doi: 10.15252/emmm.201910865
- Li G, Zhao H, Cheng Z, Liu J, Li G, Guo Y. Single-cell transcriptomic profiling of heart reveals ANGPTL4 linking fibroblasts and angiogenesis in heart failure with preserved ejection fraction. *J Adv Res*. 2024;S2090-1232(24)00068-7. doi: 10.1016/j.jare.2024.02.006

27. Heineke J, Auger-Messier M, Xu J, Oka T, Sargent MA, York A, Klevitsky R, Vaikunth S, Duncan SA, Aronow BJ, et al. Cardiomyocyte GATA4 functions as a stress-responsive regulator of angiogenesis in the murine heart. *J Clin Invest*. 2007;117:3198–3210. doi: 10.1172/JCI32573
28. Forte E, Daigle S, Rosenthal NA. Protocol for isolation of cardiac interstitial cells from adult murine hearts for unbiased single cell profiling. *STAR Protoc*. 2020;1:100077. doi: 10.1016/j.xpro.2020.100077
29. Travers JG, Wennersten SA, Pena B, Bagchi RA, Smith HE, Hirsch RA, Vanderlinden LA, Lin YH, Dobrinskikh E, Demos-Davies KM, et al. HDAC inhibition reverses preexisting diastolic dysfunction and blocks covert extracellular matrix remodeling. *Circulation*. 2021;143:1874–1890. doi: 10.1161/CIRCULATIONAHA.120.046462
30. Dobaczewski M, Chen W, Frangogiannis NG. Transforming growth factor (TGF)-beta signaling in cardiac remodeling. *J Mol Cell Cardiol*. 2011;51:600–606. doi: 10.1016/j.yjmcc.2010.10.033
31. Khalil H, Kanisicak O, Prasad V, Correll RN, Fu X, Schips T, Vagnozzi RJ, Liu R, Huynh T, Lee SJ, et al. Fibroblast-specific TGF-beta-Smad2/3 signaling underlies cardiac fibrosis. *J Clin Invest*. 2017;127:3770–3783. doi: 10.1172/JCI94753
32. Ko T, Nomura S, Yamada S, Fujita K, Fujita T, Satoh M, Oka C, Katoh M, Ito M, Katagiri M, et al. Cardiac fibroblasts regulate the development of heart failure via Htra3-TGF-beta-IGFBP7 axis. *Nat Commun*. 2022;13:3275. doi: 10.1038/s41467-022-30630-y
33. Koitabashi N, Danner T, Zaiman AL, Pinto YM, Rowell J, Mankowski J, Zhang D, Nakamura T, Takimoto E, Kass DA. Pivotal role of cardiomyocyte TGF-beta signaling in the murine pathological response to sustained pressure overload. *J Clin Invest*. 2011;121:2301–2312. doi: 10.1172/JCI44824
34. Tong D, Schiattarella GG, Jiang N, May HI, Lavandro S, Gillette TG, Hill JA. Female sex is protective in a preclinical model of heart failure with preserved ejection fraction. *Circulation*. 2019;140:1769–1771. doi: 10.1161/CIRCULATIONAHA.119.042267
35. Arroyo N, Villamayor L, Diaz I, Carmona R, Ramos-Rodriguez M, Munoz-Chapuli R, Pasquali L, Toscano MG, Martin F, Cano DA, et al. GATA4 induces liver fibrosis regression by deactivating hepatic stellate cells. *JCI Insight*. 2021;6:e150059. doi: 10.1172/jci.insight.150059
36. Mathison M, Singh VP, Sanagasetti D, Yang L, Pinnamaneni JP, Yang J, Rosengart TK. Cardiac reprogramming factor Gata4 reduces postinfarct cardiac fibrosis through direct repression of the profibrotic mediator snail. *J Thorac Cardiovasc Surg*. 2017;154:1601–1610.e3. doi: 10.1016/j.jtcvs.2017.06.035
37. Rurik JG, Tombacz I, Yadegari A, Mendez Fernandez PO, Shewale SV, Li L, Kimura T, Soliman OY, Papp TE, Tam YK, et al. CAR T cells produced in vivo to treat cardiac injury. *Science*. 2022;375:91–96. doi: 10.1126/science.abm0594
38. Zhou H, Yang J, Srinath C, Zeng A, Wu J, Leon EC, Qureshi TN, Reid CA, Nettesheim ER, Xu E, et al. Improved cardiac function in postischemic rats using an optimized cardiac reprogramming cocktail delivered in a single novel adeno-associated virus. *Circulation*. 2023;148:1099–1112. doi: 10.1161/circulationaha.122.061542
39. Mizuno-Iijima S, Ayabe S, Kato K, Matoba S, Ikeda Y, Dinh TTH, Le HT, Suzuki H, Nakashima K, Hasegawa Y, et al. Efficient production of large deletion and gene fragment knock-in mice mediated by genome editing with Cas9-mouse Cdt1 in mouse zygotes. *Methods*. 2021;191:23–31. doi: 10.1016/j.jymeth.2020.04.007
40. Tanimoto Y, Mikami N, Ishida M, Iki N, Kato K, Sugiyama F, Takahashi S, Mizuno S. Zygote microinjection for creating gene cassette knock-in and flox alleles in mice. *J Vis Exp*. 2022;184. doi: 10.3791/64161
41. Acharya A, Baek ST, Banfi S, Eskiocak B, Tallquist MD. Efficient inducible Cre-mediated recombination in Tcf21 cell lineages in the heart and kidney. *Genesis*. 2011;49:870–877. doi: 10.1002/dvg.20750
42. Zacchigna S, Paldino A, Falcao-Pires I, Daskalopoulos EP, Dal Ferro M, Vodret S, Lesizza P, Cannata A, Miranda-Silva D, Lourenco AP, et al. Towards standardization of echocardiography for the evaluation of left ventricular function in adult rodents: a position paper of the ESC Working Group on Myocardial Function. *Cardiovasc Res*. 2021;117:43–59. doi: 10.1093/cvr/cvaa110
43. Pacher P, Nagayama T, Mukhopadhyay P, Batkai S, Kass DA. Measurement of cardiac function using pressure-volume conductance catheter technique in mice and rats. *Nat Protoc*. 2008;3:1422–1434. doi: 10.1038/nprot.2008.138
44. Babicki S, Arndt D, Marcu A, Liang Y, Grant JR, Maciejewski A, Wishart DS. Heatmapper: web-enabled heat mapping for all. *Nucleic Acids Res*. 2016;44:W147–W153. doi: 10.1093/nar/gkw419
45. Zhou Y, Zhou B, Pache L, Chang M, Khodabakhshi AH, Tanaseichuk O, Benner C, Chanda SK. Metascape provides a biologist-oriented resource for the analysis of systems-level datasets. *Nat Commun*. 2019;10:1523. doi: 10.1038/s41467-019-09234-6
46. Hao Y, Hao S, Andersen-Nissen E, Mauck WM 3rd, Zheng S, Butler A, Lee MJ, Wilk AJ, Darby C, Zager M, et al. Integrated analysis of multimodal single-cell data. *Cell*. 2021;184:3573–3587.e29. doi: 10.1016/j.cell.2021.04.048
47. Shao X, Taha IN, Clauser KR, Gao YT, Naba A. MatrisomeDB: the ECM-protein knowledge database. *Nucleic Acids Res*. 2020;48:D1136–D1144. doi: 10.1093/nar/gkz849
48. Jin S, Guerrero-Juarez CF, Zhang L, Chang I, Ramos R, Kuan CH, Myung P, Plikus MV, Nie Q. Inference and analysis of cell-cell communication using CellChat. *Nat Commun*. 2021;12:1088. doi: 10.1038/s41467-021-21246-9
49. Kurotsu S, Sadahiro T, Harada I, Ieda M. A biomimetic hydrogel culture system to facilitate cardiac reprogramming. *STAR Protoc*. 2022;3:101122. doi: 10.1016/j.xpro.2022.101122
50. Robinson JT, Thorvaldsdottir H, Winckler W, Guttman M, Lander ES, Getz G, Mesirov JP. Integrative genomics viewer. *Nat Biotechnol*. 2011;29:24–26. doi: 10.1038/nbt.1754